Vol. 306: 17–30, 2006 | MARINE ECOLOGY PROGRESS SERIES
Mar Ecol Prog Ser | Published January 11

FEATURE ARTICLE

Modelling growth of Antarctic krill. II. Novel approach to describing the growth trajectory

Steven G. Candy*, So Kawaguchi

Australian Antarctic Division, Department of Environment and Heritage, 203 Channel Highway, Kingston, Tasmania 7050, Australia

ABSTRACT: Von Bertalanffy (VB) growth models for Antarctic krill have been calibrated from population-level data consisting of modal lengths obtained from a time sequence of length frequency samples. We developed an alternative approach to predicting the trajectory of length over time, using a step-growth function that combines models of instantaneous growth rate (IGR) at moult calibrated from direct measurements of individual pre- and post-moult krill sampled from the wild with a model of temperature-dependent inter-moult period (IMP). Using summer and early autumn data for juveniles and males sampled from the Indian Ocean sector of the Southern Ocean, we modelled IGR as a function of pre-moult length and season using linear mixed models (LMM) incorporating cubic smoothing splines. We generated a number of growth trajectories starting from an Age 1+ yr mean length, for different scenarios of winter and spring growth. We then provided convenient parametric approximations to these step trajectories for use in population dynamic modelling systems using either a punctuated-growth model based on an *F*-distribution or a seasonal-growth VB model. Alternatively, step-trajectories could be used directly. Our models indicated that, when allowing for shrinkage, at the start of the sixth winter after hatch (Age 5+ yr) the mean length of krill for the Indian Ocean sector was close to 53 mm, compared to 56 mm obtained from studies for the southwest Atlantic Ocean sector. In contrast, when shrinkage was not allowed for, a slightly higher mean length was obtained for krill from the Indian Ocean sector (57.5 mm) compared to krill from the southwest Atlantic Ocean sector.

KEY WORDS: Antarctic Krill · Growth · Instantaneous growth rate · IGR · CCAMLR

INTRODUCTION

Accurate characterisation and quantification of the growth of Antarctic krill *Euphausia superba* in the wild is an important research priority for this keystone species of the Antarctic marine ecosystem. Growth models that show the trajectory of total length (TL) with age are required for assessing yield of fish stocks. The growth model used in the present assessment of long-term annual yield of Antarctic krill (CCAMLR 2000), which uses the generalized yield model (GYM) and software (Constable & de la Mare 1996, 2003), is the punctuated-growth version of the von Bertalanffy (VB) growth model described by Rosenberg et al. (1986). This VB model and the seasonal VB model of Siegel (1986) were calibrated using age-cohort modal lengths estimated from length frequency data (LFD), where LFD consists of numbers of individuals in length classes sampled from catches obtained from research survey cruises. There are a number of well-known difficulties associated with estimating population-level growth from LFD, which are discussed later in this study.

An alternative source of data on the growth of wild krill has been the measurement of instantaneous growth rate (IGR) as described in Kawaguchi et al. (2006, this volume), which measures the increase in uropod length at moulting for specimens collected in the wild and individually maintained until they moult. Growth is measured by comparing the length of the uropod on the moulted exoskeleton to that on the post-moult animal. IGR is expressed as a relative value by dividing the length increment by the pre-moult length. Therefore, strictly speaking, IGR is a relative instantaneous growth rate. The growth in total length of the animal is assumed to be in the same proportion as the measured IGR for the uropods

*Email: steve.candy@aad.gov.au

(Nicol et al. 1992, Ross et al. 2000, Kawaguchi et al. 2006). Krill moult throughout their lifespan and can increase or decrease in length, or stay the same size at each moult (Ikeda & Dixon 1982, Buchholz 1991, Quetin & Ross 1991, Nicol et al. 1992). Therefore, growth rates (mm d^{-1}) are the combination of the growth increments at moulting and the moulting frequency (Ross et al. 2000).

To provide a time scale for our growth model we used inter-moult period (IMP = I), which is predicted from seasonal sea-surface temperature (T) using models of T and I as described in Kawaguchi et al. (2006). Our model of IGR uses the statistical model fitting techniques described in Kawaguchi et al. (2006) but with the model calibrated using a subset of their data. This involved fitting a linear mixed model (LMM) incorporating cubic smoothing splines to model smooth trends in IGR with pre-moult length and with season. Kawaguchi et al. (2006) presented IGR data for 2 regions of the Southern Ocean, the Indian Ocean sector and the southwest Atlantic sector, but the majority of data came from the former region with mean IGR estimated with poor precision for the latter. For this reason, we calibrated our model of IGR using only data from the Indian Ocean sector (see Kawaguchi et al. 2006, their Fig. 1). In addition, Kawaguchi et al. (2006) found significant differences between larger males and females in mean IGR for krill collected in January and February, which is after the peak phytoplankton bloom that occurs in December in the Indian Ocean sector. The decrease in growth for females was inferred to be due to the diversion of resources by females into reproductive processes at the expense of somatic growth. To avoid this complexity we modelled IGR only for juveniles and males, and we discuss the implications of sex differences in growth on the definition of 'population-average' with respect to growth trajectories.

A starting mean length is required to project the modelled length through time, and IMP was predicted given a starting date of 1 May using the models for T and I and a technique commonly used in predicting insect emergence dates (Stinner et al. 1974, 1975, Dallwitz & Higgins 1992). We then compared our step-projection model with existing VB curves and estimated both punctuated growth (Rosenberg et al. 1986) and seasonal growth (Siegel 1986) versions of the VB model using the IGR/IMP trajectory.

The aims of this study were therefore to (1) generate a step growth trajectory model based on models of IGR and IMP, (2) provide convenient parametric approximations to the step trajectory using either a punctuated-growth model or a seasonal-growth VB model, (3) compare this with the existing krill growth models, (4) discuss the implications of our model for resource management, and finally (5) recommend studies, both in the field and in captive rearing conditions, that are required to improve our model.

METHODS

IGR model. A subset of the data described by Kawaguchi et al. (2006) was used whereby only males and juveniles from the Indian Ocean sector were used for model fitting. The statistical methods and models used in this study, involving LMMs and cubic smoothing splines (Verbyla et al. 1999, Butler et al. 2002), were the same as those in Kawaguchi et al. (2006) except where noted otherwise. The predicted means for each combination of maturity (male, juvenile), month of capture, and pre-moult total length class (TLC) (classes were 4 mm wide between 16 and 52 mm, with first and last classes of 8 to 16 mm and 52 to 60 mm, respectively), adjusted for days from capture to moult using a smoothing spline in the variable Dm1 (days from capture minus 1) as described in Kawaguchi et al. (2006), were obtained from the LMM.

In order to predict a population-average krill growth trajectory, a LMM incorporating 2 cubic smoothing splines in addition to the spline in Dm1 was used. One spline was used to model the trend in IGR with size. In Kawaguchi et al. (2006), the cubic smoothing spline for size used the mean pre-moult total length for each TLC, termed TLCL; however, here we used the inverse of these means (ITLCL = $TLCL^{-1}$) since we could then compare the spline model with a simpler model using only linear terms in ITLCL. The other differences in spline terms in the LMM, compared to those used by Kawaguchi et al. (2006), were that (1) maturity (juvenile versus male) was not considered as a predictive factor in the spline terms for either ITLCL or Dm1, but that data for both males and juveniles were used in the fit in order to provide IGR values for the maximum range of size classes possible, and (2) in order to allow prediction of IGR for any time point rather than only for nominal months of sampling, a cubic smoothing spline was used to model the trend in the slope of the IGR to ITLCL relationship with month. To do this, months were given nominal numeric values of $M^{(IGR)} = 1, \ldots, 5$ for December to April, respectively. A simple linear relationship between the regression intercepts for the month-specific regressions and $M^{(IGR)}$ was also included in the LMM.

The random effects were as described in Kawaguchi et al. (2006). All predictions of IGR were obtained by back-transforming predictions from the LMMs: log transformed values of IGR (with adjustment for negative values) were fitted by the LMMs as described by Kawaguchi et al. (2006).

Prediction of a population-average krill growth trajectory. To predict the growth trajectory, the model of IGR was combined with the models described in Kawaguchi et al. (2006) for IMP and average sea surface temperature seasonal trend in the Indian Ocean sector. To predict IMP under fluctuating temperatures in the natural environment, we applied a technique commonly used to predict insect development times in the field (Stinner et al. 1974) that employs development rate models calibrated from constant-temperature rearing studies. The steps involved in projecting growth in TL from an assumed starting premoult TL value, to provide a predicted growth trajectory from models of IGR and IMP, were given by the following growth projection algorithm:

Step 1. Assuming a starting date of 1 May, IMP (I) was predicted using predicted temperatures from the model of sea surface temperature given by Kawaguchi et al. (2006):

$$I = \exp[\beta_0 + \beta_1 \ln(T+2)] \quad (1)$$

$$\ln(T+2) = \alpha_0 + \frac{\alpha_1}{2\pi}\sin[2\pi(M/12-\alpha_2)] \quad (2)$$

where T is sea surface temperature (°C), M is month number (i.e. May = 1, June = 2, …, April = 12), and parameter estimates obtained from Kawaguchi et al. (2006) were $\beta_0 = 3.5371$, $\beta_1 = -0.5358$, $\alpha_0 = -0.3609$, $\alpha_1 = -8.4089$, and $\alpha_2 = 0.0512$. To implement Eq. (2), day of the year (i.e. 1 to 365 from 1 May) for each of 5 yr was generated and converted to a value of M_i between 1 and 13 (i.e. 1 = 1 May, 13 = 30 April) for day i = 1, ..., 1825 and then used to predict T_i. For each day from 1 to 1825, the fractional development, D_i (Stinner et al. 1974) up to that day was obtained by the formula:

$$D_i = \sum_{i'=1}^{i}\{\exp[\beta_0+\beta_1\ln(T_{i'}+2)]\}^{-1}$$

where the days on which moults were predicted to occur were taken to be days when D_i was closest to the set of integers j = 1, 2, 3, ..., N. The largest integer value of D_i, N, was taken to be the total number of moults over the 5 yr period, and corresponding IMPs were obtained as the difference in days between consecutive moult dates (d_j) where these dates were expressed in days from 1 to 1825 and given by:

$$d_j = \sum_{i=1}^{1825}\delta[(D_i+0.0001)\le j]$$

where the δ is an indicator function which takes the value 1 if the argument is true and 0 if false, and the addition of 0.0001 to D_i is used to overcome finite computer numerical precision.

Step 2. The moult dates (d_j; j = 1,..., N) were converted to a month and fraction of month of the year between 1 and 13, ignoring the year for the purposes of predicting IGR at moult date. These values of M_j (j = 1, ..., N) were translated from the 1 May to 31 April scale to the relevant date scale for IGR from 1 December to 31 November, to give $M_j^{(IGR)}$ (j = 1, ..., N). The IGR model only covered the period from December to April and, since spline models cannot be extrapolated to any great degree, other strategies were adopted to compute an estimated IGR for the winter and spring period from May to November. These strategies called 'scenarios' are given in the results section. Given the short observation period from December to April, even a cyclical model such as Eq. (2) was not useful for this purpose; furthermore, a nonlinear model such as this does not fit into the LMM framework.

Step 3. Given the values $M_j^{(IGR)}$ (j = 1, ..., N) the population-average TL was calculated by starting with an assumed mean TL of 28 mm for 1 yr old krill as of 1 May in Year 1 of the projection (we also investigated the effect of using 26 and 30 mm starting mean lengths). The IGR was predicted from the LMM using the 'predict' function from the SAMM (Spatial Analysis Mixed Models with S-plus) suite of functions (Butler et al. 2002) given this value of TL and the value of $M_j^{(IGR)}$. The predicted IGR was multiplied by TL to give a growth increment which was then added to the (premoult) TL. This incremented value of TL was used in the next growth period between first and second moults, and this process was repeated for the full 5 yr period. So that the arbitrary starting date of 1 of May would not overly influence the predicted trajectory, the IGR prediction for moult j was not in fact the value given $M_j^{(IGR)}$ but rather the average value of the set of predicted IGRs for all days, converted to months, between moults $j-1$ and j; however, updates of TL were not carried out in daily steps but only at the moult dates. The trajectory for TL, assuming growth increments to be instantaneous pulses of growth at moult times, is therefore a step function rather than a smooth curve such as the VB growth curve.

Calibrating a VB growth model from IGR and IMP models. Various VB based growth curves have been used in the past to model the growth trajectory of krill (Pauly & Gaschutz 1979, Rosenberg et al. 1986, Siegel 1986). The VB growth model for TL (L) and age (A) is given by:

$$L = L_\infty\{1 - \exp[-\kappa(A-t_0)]\} \quad (3)$$

where the parameters of the VB model are the upper asymptote L_∞, location parameter t_0, and the rate parameter κ. The relative IGR derived from Eq. (3) is given by:

$$\frac{1}{L}\frac{dL}{dA} = -\kappa + \kappa L_\infty\frac{1}{L}$$

If we assume that IGR is equivalent to $L^{-1}\cdot dL/dA$ it is tempting to think that if we also assume t_0 to be 0, as in

Rosenberg et al. (1986), then we can estimate the VB parameters directly from the IGR data by fitting a linear regression of IGR on inverse of length:

$$\mathrm{IGR} = \beta_0 + \beta_1 \frac{1}{L}$$

and recovering the VB parameters by the relations $\kappa = -\beta_0$ and $L_\infty = \beta_1/-\beta_0$. However, it is well known—as was demonstrated by Kawaguchi et al. (2006)—that IGR is not only highly dependent on length but is also highly dependent on season, which Eq. (3) does not take into account.

A VB model incorporating seasonal growth (SVB) is given by (Siegel 1986):

$$L = L_\infty\left(1 - \exp\left[-\left\{\kappa(A-t_0)+\frac{\theta_0\kappa}{2\pi}\sin\left[2\pi(A-\theta_1)\right]\right\}\right]\right) \quad (4)$$

where θ_0 and θ_1 are extra parameters to be estimated simultaneously with the usual VB parameters.

There is no simple equivalent expression for $L^{-1}\cdot \mathrm{d}L/\mathrm{d}A$ from Eq. (4) that is a function only of L and VB parameters as there is for Eq. (3). Therefore, in order to fit Eq. (4) using the IGR data and since we cannot use IGR directly, we fitted Eq. (4) to the growth trajectory obtained from the growth projection algorithm, where predicted values of TL immediately after moult were used as 'pseudo-data' for L, and age at moult was used to give A where A is years from hatch assuming hatch date to be 1 December.

An alternative to Eq. (4), which incorporates a period of zero growth within the year (i.e. late autumn/winter/spring) combined with a VB growth curve for the part of the year when growth is positive (summer/early autumn), is more complex to calibrate than Eq. (4). Rosenberg et al. (1986) fitted such a model using monthly LF data and derived a step function for the length trajectory with a punctuated-growth VB (PVB) model. Given an assumed fraction of the year g, for which growth is assumed to occur, they specified a PVB model derived from Eq. (3) where $\kappa' = \hat{\kappa}/g$ to give the following step function:

$$\begin{aligned} L &= L_\infty\left[1-\exp\{-\kappa'[A-n(1-g)]\}\right]; && n < A \le n+g \\ &= L_{n+g}; && n+g < A < n+1 \end{aligned} \quad (5)$$

where n is the number of winters that krill have survived. Rosenberg et al. (1986) used a value for g of 0.25, assuming the year starts at 1 December. The present assessment of long-term annual yield of Antarctic krill (CCAMLR 2000) uses Eq. (5) with parameter values $L_\infty = 60$, $\kappa = 0.45$, $t_0 \equiv 0$ from Rosenberg et al. (1986). We found that the PVB model, calibrated to the length trajectory 'pseudo-data', could not adequately reproduce this trajectory. For this reason, we described a periodic growth model using final or asymptotic lengths for each no-growth period and length in the growth-period, predicted using a scaled cumulative F-distribution as described by the following equation:

$$\begin{aligned} L &= L_{\infty,n} + F_{50,50}(\beta M_F / g^\star)(L_{\infty,n+1} - L_{\infty,n}); && 1 < n+g_0-1 < A \le n+g_1 \\ &= L_{\infty,n}; && n+g_1 < A \le n+g_0-1,\ A>1 \end{aligned} \quad (6)$$

where we define A as age in years (starting from 1 December); $M_F = M^\star + \delta - g_0$, where $M^\star = A - int(A)$ and $int(A)$ is the integer value of age; $g_1 = M^\star_{30\mathrm{Apr}} = 0.4137$; $g_0 = M^\star_{30\mathrm{Sep}} = 0.8329$ (i.e. sum of days across months from 1 December divided by 365); $\delta = 1$; $A \ge 2 \cap M^\star < g_0$ (= 0, otherwise); $g^\star = (1 + g_1 - g_0)/2$; $F_{50,50}(x)$ as the cumulative density of the F-distribution with 50 numerator and 50 denominator degrees of freedom for an ordinate value of x; β as a scale parameter to be estimated; and asymptotes $L_{\infty,n}$ obtained by noting the mean length from the trajectory after n winters from hatch.

RESULTS

IGR model

Fig. 1 shows mean IGR and SE estimated from the LMM for combinations of maturity (juveniles versus males), month, and TLC. Fig. 1 also shows 3 sets of cubic spline models (a,b,c) for each of 5 mo from December to April and corresponding to the following LMMs: LMM_a: month-specific slopes for the linear term in ITLCL combined with a smoothing spline term in ITLCL, with intercepts a linear function of $M^{(\mathrm{IGR})}$; LMM_b: as for LMM_a except that month-specific slopes were replaced by a smoothing spline in $M^{(\mathrm{IGR})}$; and LMM_c: as for LMM_a except that the smoothing spline term in ITLCL was dropped. Fig. 1 also shows approximate 95% confidence bands for predictions from LMM_a.

Fig. 2 shows daily growth rates (mm d^{-1}) obtained from means and predictions of IGR and their SEs. Means and predictions from LMM_a, LMM_b, and LMM_c for IGR were scaled to give daily growth rates over a period of the predicted IMP for the month obtained by multiplying IGR values by TLC mean pre-moult length, and dividing by the predicted IMP for the month (see Kawaguchi et al. 2006, Table 1). In effect, this spreads the 'instantaneous' growth quantified by IGR uniformly across the period from the time of moult to which the IGR relates until the time just prior to the next moult, i.e. the relevant IMP.

It can be seen in Fig. 1 that the simple hyperbolic relationship between IGR and pre-moult TL corresponding to LMM_c is inadequate for the months January and February where the trend in means appears to involve a hyperbolic relationship with pre-moult TL for low and high TLCs, but an approximately

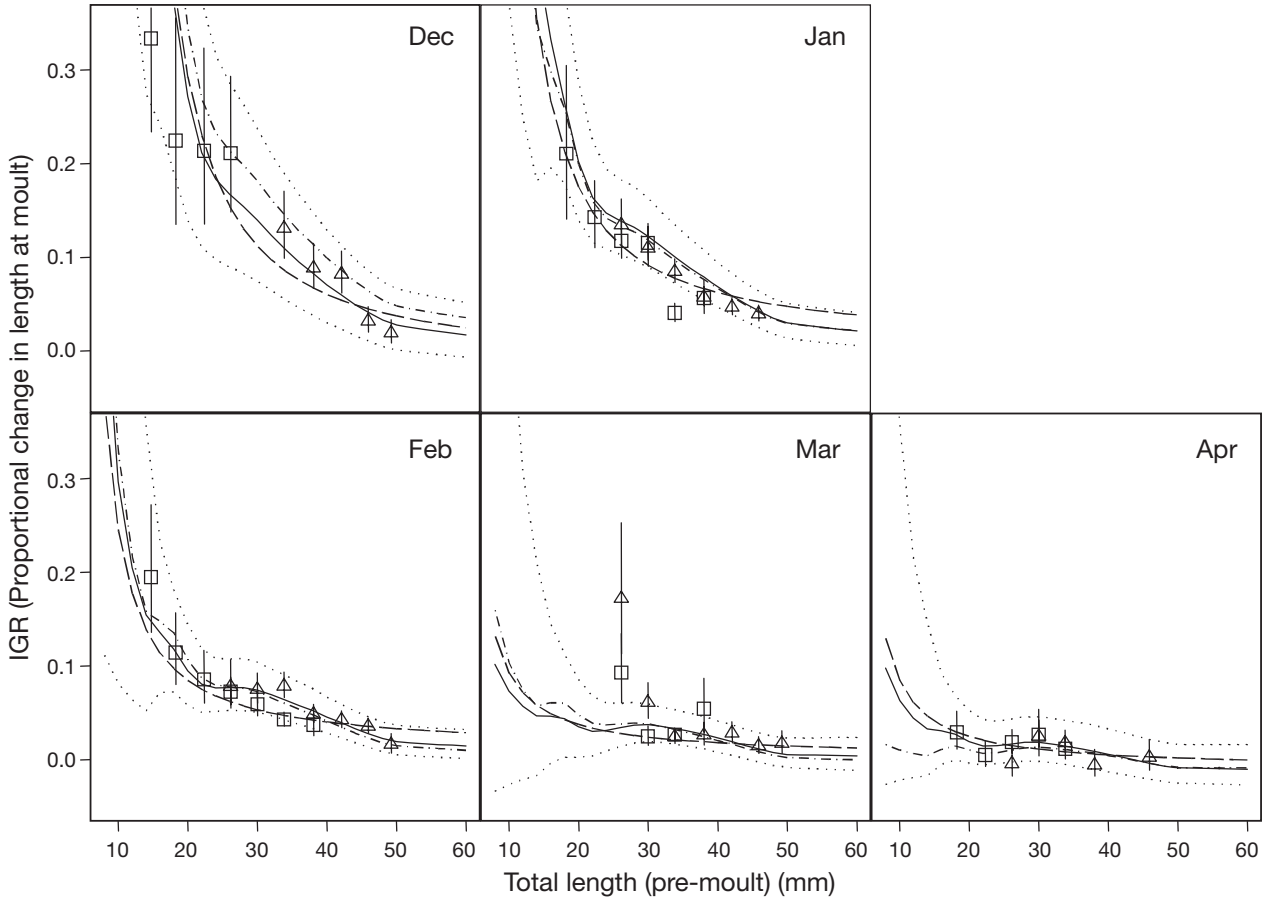

Fig. 1. *Euphausia superba*. Predicted IGR (proportional change in length at moult) against pre-moult length with SE bars and fitted spline models. Juveniles: □; males: △; LMM_a: ——— (95% confidence bounds shown as dotted lines), LMM_b: ·—·—·—; LMM_c: — — —

linear relationship for intermediate TLCs. This combination of hyperbolic and linear segments is better modelled using LMM_a and LMM_b, which involve cubic smoothing spline terms in ITLCL. The lack of fit of LMM_c for these 2 months is more dramatically demonstrated in Fig. 2. LMM_a and LMM_b give very similar fits as demonstrated in both Figs. 1 & 2. This is confirmed in Fig. 3, which shows monthly estimates of mean IGR, where month is represented by $M^{(IGR)}$, obtained by multiplying the month-specific slope estimates from LMM_a by mean pre-moult TL for the TLC of 28 to 32 mm, and the line represents the fitted cubic smoothing spline in $M^{(IGR)}$ from LMM_b. It can be seen from Fig. 3 that the correspondence of the line to the points is good, with the exception of December where the spline model over-predicts IGR. A number of different models were tried as alternatives to the spline, including a section of a sine curve and a 2nd-degree polynomial, but without significant improvement. Note that in Fig. 3 the SE bar for December is considerably larger than those for other months, which could explain the poorer fit to the point estimate for December. This is the reason for the over-prediction of mean IGR in December using LMM_b compared to LMM_a, as seen in Figs. 1 & 2. Given the uncertainty of the December estimate in Fig. 3, and the necessity of smoothing across months, predicted IGRs from LMM_b were used in Step 3 of the growth projection algorithm.

Fig. 4 shows the seasonal sea surface temperature profile from Kawaguchi et al. (2006) (Indian Ocean sector) and predicted moult dates and IMP obtained from Step 2 of the algorithm for the first year of the growth trajectory (Age 1 at 1 May to Age 2 at 1 May). Since the sum of IMPs shown in Fig. 4 does not add up exactly to 365 d, but instead to a sum of 371 d, this means that moult dates and corresponding IMPs will be slightly but progressively shifted later in each subsequent year of the 5 yr projection period.

Under ideal circumstances, year round coverage of growth rate measurements would be available to generate the growth trajectory. However, given logistical restrictions for operations in the Southern Ocean, data

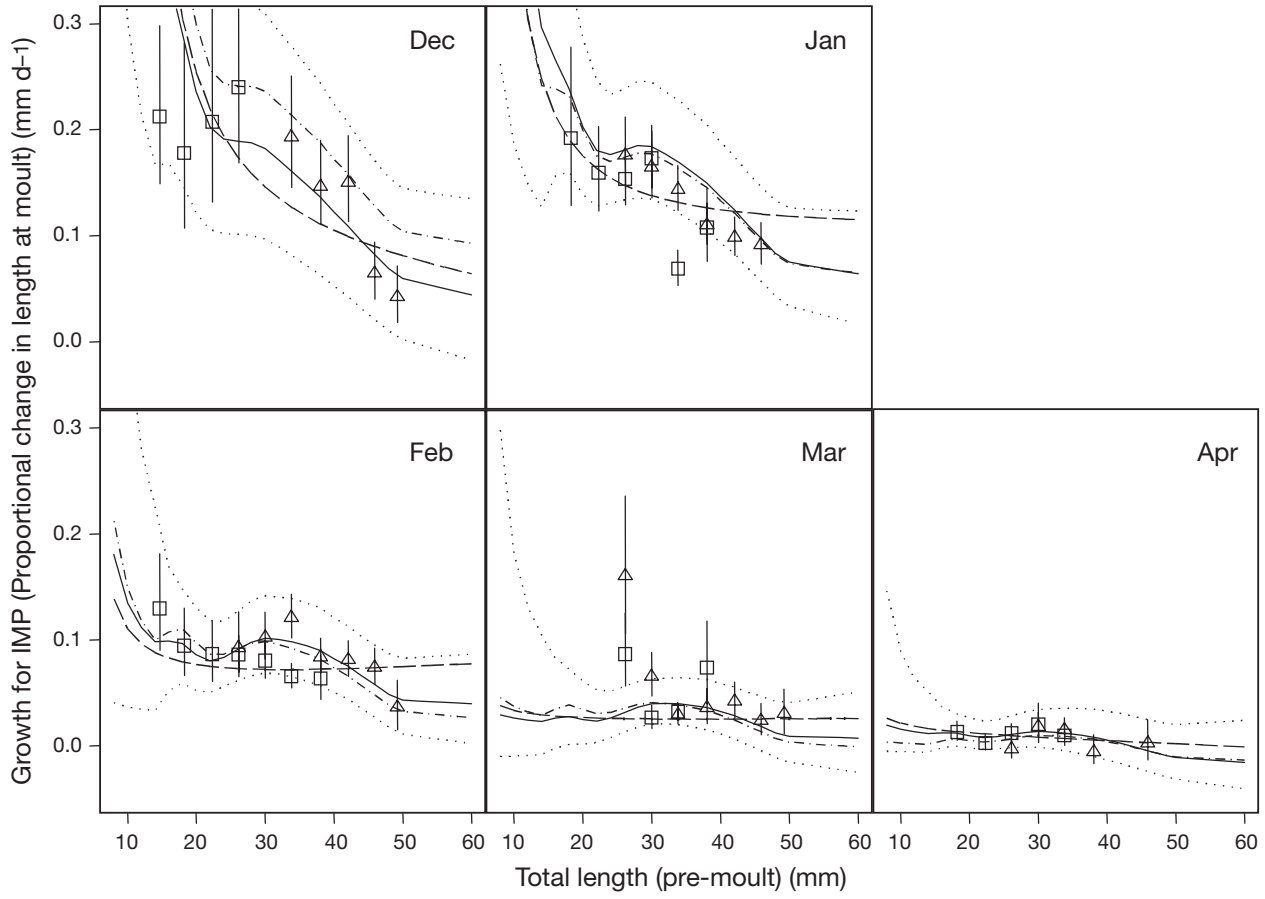

Fig. 2. *Euphausia superba*. Predicted specific growth rates (mm d^{-1}) against pre-moult length shown with SE bars and fitted spline models. Juveniles: □; males: △; LMM_a: ——— (95% confidence bounds shown as dotted lines), LMM_b: ·—·—·—; LMM_c: — — —. IMP: inter-moult period

coverage in the Indian Ocean sector was restricted to the period between December and April. Therefore, we had to extrapolate predictions from LMM_b outside these months and/or assume IGR values for the May to November period. Although cubic smoothing spline sub-models in LMM_b can be used for interpolation, they cannot in general be used for extrapolation. We used a number of strategies or 'scenarios' to predict IGR from May to November: 4 scenarios (labelled Scenario I to Scenario IV) were used along with sub-scenarios a, b, and c. Sub-scenarios dealt with how predictions of negative IGR were handled for all months. These were: (a) set negative predicted values of IGR to 0 (i.e. do not allow negative growth), (b) allow negative predictions of IGR as obtained from LMM_b, and (c) set predictions of IGR for moult dates from May to November to –0.01. For all 4 scenarios and all moult dates in the December to April period, we predicted IGR from LMM_b by calculating moult dates as month plus fraction of the month, which in effect interpolates between integer values of $M^{(IGR)}$. For example, the fourth moult occurred in Year 1 of the projection on Day 216 (Fig. 4), which fell on 2 Dec; therefore, $M^{(IGR)}$ = 1 + 2/31. However, it should be noted that for the projection algorithm, nominal dates of 1 May and 1 December could be translated to any day within each

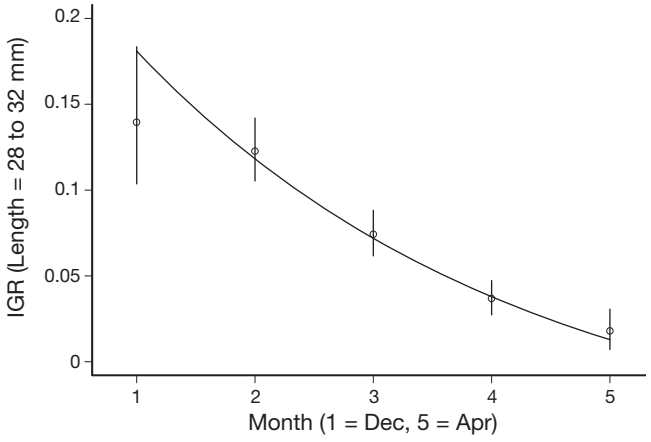

Fig. 3. *Euphausia superba*. Monthly estimates of mean instantaneous growth rate with SE bars and fitted cubic smoothing spline

calendar month (e.g. 15 May and 15 December) without affecting the results to any degree of practical significance (i.e. only the difference in days per calendar month would cause any variation in the results). The 4 scenarios determined how prediction of IGR for moult dates in the May to November period were calculated before the sub-scenario restrictions were imposed. The scenarios were:

- Scenario I: apply LMM_b prediction for April to all moult dates in the May to November period
- Scenario II: as for Scenario I, except apply LMM_b predictions as a 'mirror image' about 15 December for moult dates in November; e.g. if moult date is 15 November, use a value for $M^{(IGR)}$ = 2 + 15/30 corresponding closely to the LMM_b prediction for 15 January
- Scenario III: as for Scenario II, except extend the 'mirror image' to October (i.e. apply LMM_b predictions from February to October)
- Scenario IV: as for Scenario III except, extend the 'mirror image' to September (i.e. apply LMM_b predictions from March to September)

Therefore Scenarios I to IV progressively incorporate positive growth backwards from early summer to early spring, in a way that reflects the modelled trend in IGR throughout summer to the early autumn months.

Fig. 5 demonstrates the growth projection algorithm for Scenarios I to IV and sub-scenario a, and compares the resultant step function trajectory to the baseline VB model of Rosenberg et al. (1986) given by the VB model:

$$L = 60[1 - \exp(-0.45A)]$$

where A is age in years, the 'birth-date' of all krill is assumed to be 1 December, and t_0 is assumed 0.

From these results, it can be seen that without assigning any significant positive growth before December (Scenario Ia using predicted IGRs for April), we obtained a growth trajectory which matched the demography obtained from field surveys in the Indian Ocean sector (e.g. Pakhomov 1995). Assigning stronger positive growth to spring and early summer months via Scenarios IIa to IVa resulted in trajectories that gave mean lengths much higher than is realistic, with the Age 5+ yr over the summer growth season between 58 and 64 mm. Scenarios II to IV will therefore not be considered further.

Fig. 6 shows the growth projection algorithm for Scenario I with sub-scenarios a, b and c, and compares the resultant step function trajectory to the baseline VB model of Rosenberg et al. (1986).

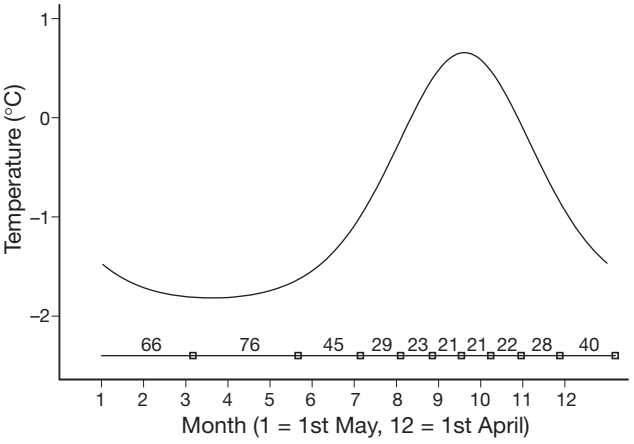

Fig. 4. Seasonal sea surface temperature and predicted intermoult period of *Euphausia superba* for start date 1 May

Scenario Ib and Ic both showed decreases in TL from April to November. Winter shrinkage was less pronounced in Scenario Ib compared to Ic for ages below 4, whereas the reverse was true for ages above 5. This was because IGR was not fixed at −0.01 for the winter/spring months in sub-scenario b. For example, LMM_b predictions of IGR for 50 mm krill was as low as −0.02 but growth was never <0 for krill less than 40 mm (Fig. 1) in contrast to Scenario Ic. For this reason, Scenario Ic will not be considered further. Mean lengths produced by Scenario Ia and Ib trajectories by the winter of the Age 5+ yr were 57.5 and 53 mm, respectively, a difference of 4.5 mm. This difference was not greatly affected by starting mean length; Fig. 7

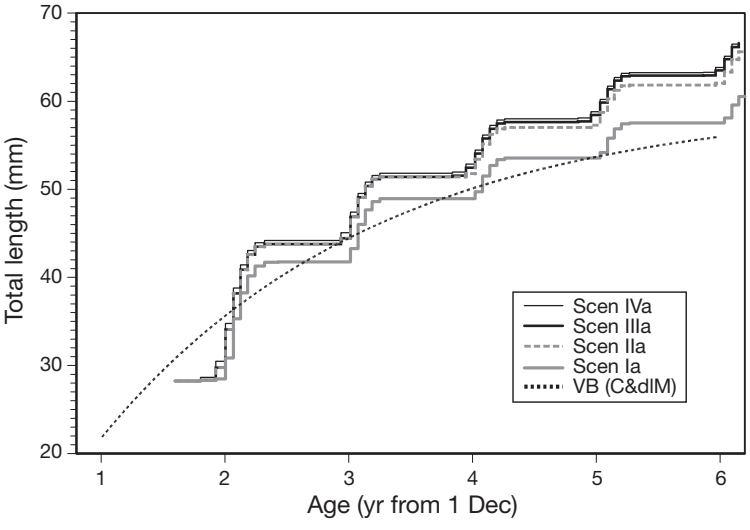

Fig. 5. *Euphausia superba*. Step-function growth trajectories for TL predicted from growth projection algorithm that combines predictions of intermoult period with instantaneous growth rate for Scenarios (Scen) I, II, III, and IV combined with sub-scenario a. Predicted trajectory from baseline VB model of Rosenberg et al. (1986) (see also Constable & de la Mare 1996) is also shown (black dashed line)

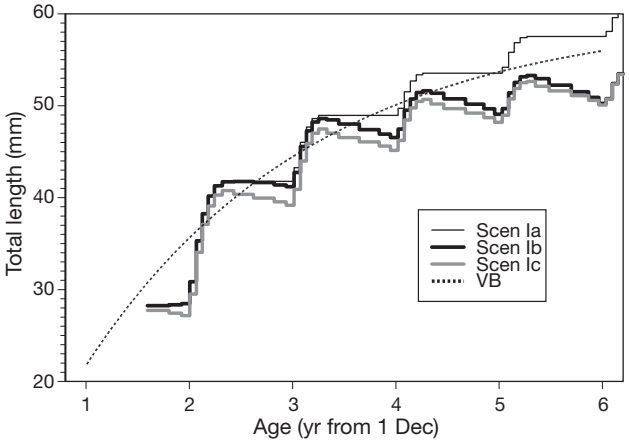

Fig. 6. *Euphausia superba*. Step-function growth trajectories for TL predicted from growth projection algorithm that combines predictions of inter-moult period with instantaneous growth rate for sub-scenarios a, b, and c combined with Scenario I. Predicted trajectory from baseline VB model of Rosenberg et al. (1986) (dashed line) is also shown

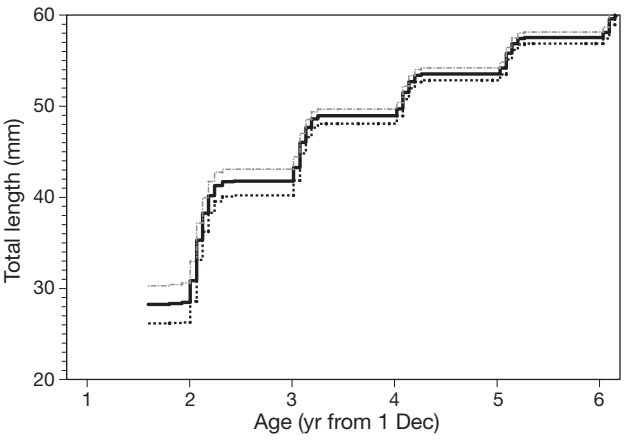

Fig. 7. *Euphausia superba*. Step-function growth trajectory for TL predicted from growth projection algorithm that combines predictions of inter-moult period with instantaneous growth rate for Scenario Ia and starting lengths 26, 28, and 30 mm

shows the Scenario Ia trajectory for starting lengths of 26, 28, and 30 mm. Interestingly, but not surprisingly, Fig. 7 shows that the 4 mm range in these starting mean lengths was gradually reduced each growth season so that by the winter of the Age 5+ yr the range was only a little over 1 mm. The same trend was obtained for Scenario Ib (not shown). Table 1 shows ranges in mean length from Ages 1+ to 5+ yr for published field data from the Indian Ocean sector, along with corresponding ranges in means from Scenarios Ia and Ib at the start of winter for each year using 26, 28, and 30 mm starting mean lengths. Table 1 shows that these 2 scenarios were in good agreement with, or had slightly higher mean lengths (particularly Scenario Ia) than, many field data from the same area.

Empirical models of the IGR/IMP trajectory

Fig. 8 shows the fit of the SVB model (Eq. 4) to the Scenario Ib trajectory in addition to the model of Siegel (1986), while Fig. 9 shows the fit of Eq. (6) to the Scenario Ia trajectory, denoted PF(Ia), along with the PVB model (Eq. 5) of Rosenberg et al. (1986). The parameter estimates for the SVB model (Eq. 4) were (with SE in brackets) $\hat{L}_\infty$ = 53.89 (0.45), $\hat{t}_0$ = 0.43 (0.09), $\hat{\kappa}$ = 0.6792 (0.0441), $\hat{\theta}_0$ = 2.519 (0.263), and $\hat{\theta}_1$ = 0.094 (0.013), while the residual mean square (RMS) was 1.0416 with 44 degrees of freedom. The estimate of β for Eq. (6) was 1.239 (95% confidence limits of 1.222 and 1.257) and the RMS was 0.0557 with 48 degrees of freedom; values of $L_{\infty,n}$ in Eq. (6) were taken directly from the Scenario Ia trajectory with values of 28.0, 41.77, 48.95, 53.55, 57.53 and 61.06 mm for Ages 1+ to 6+ yr, respectively. Since Eq. (6) fitted the Scenario Ia trajectory so well, we attempted to find a similar simple parametric model to describe the Scenario Ib trajectory; however, due to the variable-length periods of decline in length a simple model was not forthcoming. As an alternative to using predictions from Eq. (4) or Eq. (6), a table of values for Scenario Ib and Scenario Ia trajectories using 26, 28, and 30 mm starting mean lengths is provided (Table 2). Values of mean TL for any age within the range in this table can be obtained from the given values of mean length and age using linear or nonlinear interpolation.

Table 1. *Euphausia superba*. Mean length-at-age (mm) data in the Indian Ocean sector of the Southern Ocean

Season	Age yr					Source
	1+	2+	3+	4+	5+	
Dec–Mar	29.6–32.2	37.4–38.3	43.4–44.8	47.8–50.7	52.4–55.4	Aseev (1984)
Dec–Feb	19.0–30.8	34.2–40.9	41.2–48.8	51.0–54.9		Hosie et al. (1988)
Jan–Feb	22.3–28.4	39.0–41.8	44.2–46.4	49.2–55.0	54.8	Wang et al. (1995)
Mar–Apr	25.7–30.6	32.8–40.7	40.3–48.3	49.2–55.0		Pakhomov (1995)
Mar–Apr	28.4	41.8	46.4	50.3	54.8	Lu & Wang (1996)
Dec–Mar	26.0–30.0	40.0–43.0	48.0–49.5	53.0–54.0	57.0–58.0	This study (Scenario Ia)
Dec–Mar	26.0–30.0	40.0–43.0	48.0–49.5	51.0–52.0	53.0–54.0	This study (Scenario Ib)

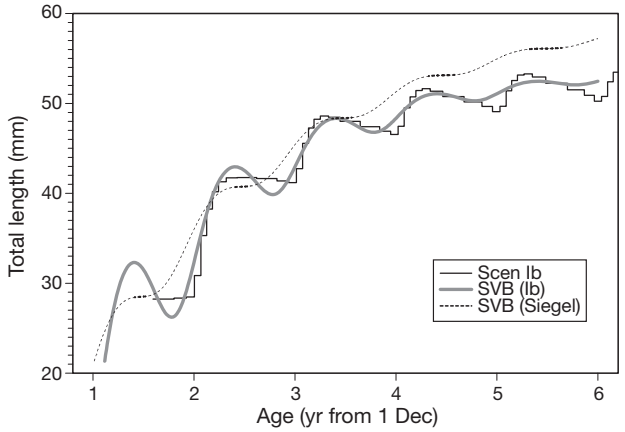

Fig. 8. *Euphausia superba*. Step-function growth trajectory for TL predicted from growth projection algorithm that combines predictions of inter-moult period with instantaneous growth rate for Scenario Ib. Predicted trajectories for SVB models fitted either to step-trajectory Scenario Ib or as in Siegel (1986) (dashed line) are also shown

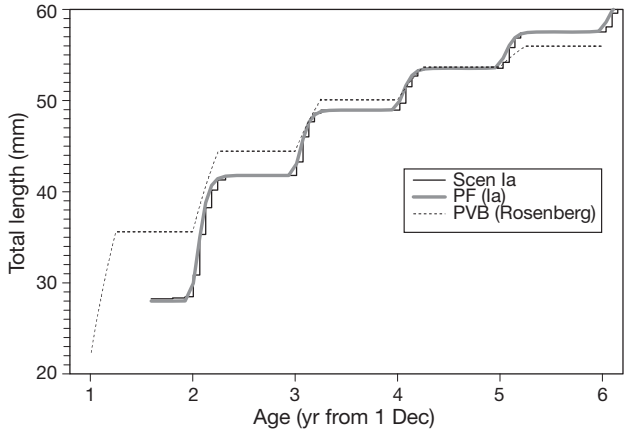

Fig. 9. *Euphausia superba*. Step-function growth trajectory for TL predicted from growth projection algorithm that combines predictions of inter-moult period with instantaneous growth rate for Scenario Ia. Predicted trajectories for PVB growth model of Rosenberg et al. (1986) (dashed line) and punctuated *F*-distribution model PF(Ia) are also shown

DISCUSSION

IGR generated growth trajectories

Allowing little or no growth in November as in Scenario Ia is probably realistic: it reflects the fact that, although mature krill are usually observed throughout December to February and therefore should have already started intensive energy accumulation before this time, the net result of the energetic budget has not allowed significant somatic growth to occur. In support of this conclusion, krill are thought to be dependent on sea ice algae for food when they do not have enough food available in the water column during spring, so that the method of feeding, abundance, and calorific value of this food source may only allow maintenance of those basic body functions required for survival. It is questionable whether the spring phytoplankton bloom occurs in November in the Indian Ocean sector (Jacques & Fukuchi 1994); however, Grose & McMinn (2003) observed reasonable density of the under-ice algal community in the winter season, which rapidly increases from November. This could potentially be a major food source for krill in early spring in the pack ice zone in the eastern Antarctic.

Fig. 6 demonstrates that when negative predictions of IGR were allowed in sub-scenarios b and c by the end of summer for Age 5+ yr krill, mean length was 4 to 5 mm shorter than if negative predictions of growth were set to 0. An assumption of May to November IGR of −0.01 for all size classes was probably unrealistic because it gave negative growth for krill less than 45 mm in length, which was not supported by means or spline curves shown in Figs. 1 & 2. There is an ongoing debate as to whether krill generally shrink in size during winter when food is scarce under natural conditions. Long-term laboratory experiments have proven that krill do shrink in size when starved and can live for over 200 d without feeding, and shrinkage was suggested to be one possible over-wintering strategy (Ikeda & Dixon 1982). Quetin & Ross (1991) demonstrated evidence of shrinkage of up to 2% per moult during winter through field IGR measurements. Our IGR prediction for April also showed as much as 1.5% shrinkage at 50 mm size, which strongly supported the idea that shrinkage at this level is a general phenomena that occurs in the winter season (Kawaguchi et al. 2006).

Allowing for this general level of winter shrinkage (Senario Ib) gave a trajectory for mean length that showed reasonable agreement with field demography reported in the past (Table 1), whereas the trajectory generated without any winter shrinkage (Scenario Ia) followed the higher end of the range of field observations of size ranges at each age.

Another factor to be considered is the relationship between IMP and feeding conditions. It is well known that IMP is not only a function of temperature but can be prolonged by starvation (Buchholz 1991). Data coverage of IGR during winter, in addition to a further understanding of IMP, is crucial to the improvement of model predictions of winter growth. This study is the first attempt to see the actual effect of the level of shrinkage observed from field IGR on the mean growth trajectory. Since Scenario Ib is the scenario consistent with observed IGR, and is also consistent with winter information from previous studies (Quetin & Ross 1991, Quetin et al. 1994) and provides reasonable length-at-age estimation, we believe this to be the best model among all scenarios.

Table 2. *Euphausia superba*. Predictions of mean total length (TL) using Scenarios Ia and Ib for initial TL 26, 28 and 30 mm

Projection Period[a] (d)	Age from birth[b] (yr)	Scenario Ia			Scenario Ib		
		26 mm	28 mm	30 mm	26 mm	28 mm	30 mm
66	1.59	26.16	28.24	30.28	26.16	28.24	30.28
142	1.80	26.20	28.35	30.43	26.19	28.34	30.43
187	1.93	26.27	28.48	30.60	26.24	28.48	30.60
216	2.01	28.58	30.86	32.97	28.54	30.86	32.97
239	2.07	33.14	35.30	37.18	33.11	35.30	37.18
260	2.13	36.24	38.24	39.96	36.21	38.24	39.96
281	2.18	38.30	40.18	41.74	38.27	40.17	41.74
303	2.24	39.54	41.28	42.73	39.52	41.28	42.73
331	2.32	40.08	41.72	43.07	40.05	41.72	43.07
371	2.43	40.21	41.77	43.08	40.18	41.77	43.04
441	2.62	40.21	41.77	43.08	40.14	41.65	42.85
514	2.82	40.21	41.77	43.08	39.93	41.38	42.51
556	2.94	40.21	41.77	43.08	39.80	41.18	42.26
584	3.01	41.85	43.27	44.44	41.47	42.73	43.71
607	3.08	44.82	46.02	47.01	44.49	45.56	46.38
628	3.13	46.62	47.67	48.54	46.33	47.27	48.00
648	3.19	47.65	48.60	49.39	47.39	48.24	48.89
671	3.25	48.07	48.94	49.68	47.84	48.61	49.21
700	3.33	48.09	48.95	49.68	47.74	48.46	49.02
742	3.45	48.09	48.95	49.68	47.33	48.00	48.52
815	3.65	48.09	48.95	49.68	46.76	47.40	47.89
885	3.84	48.09	48.95	49.68	46.31	46.91	47.37
925	3.95	48.09	48.95	49.68	45.98	46.54	46.97
952	4.02	48.92	49.71	50.41	46.96	47.46	47.84
974	4.08	50.77	51.51	52.20	49.08	49.51	49.84
995	4.14	51.98	52.70	53.37	50.33	50.73	51.06
1016	4.20	52.65	53.37	54.03	51.03	51.43	51.75
1039	4.26	52.84	53.55	54.20	51.23	51.63	51.95
1068	4.34	52.84	53.55	54.20	50.97	51.36	51.67
1113	4.46	52.84	53.55	54.20	50.37	50.76	51.07
1190	4.67	52.84	53.55	54.20	49.78	50.17	50.47
1255	4.85	52.84	53.55	54.20	49.28	49.66	49.97
1293	4.96	52.84	53.55	54.20	48.71	49.08	49.38
1320	5.03	53.48	54.18	54.83	49.35	49.69	49.97
1342	5.09	55.12	55.81	56.44	51.08	51.41	51.68
1362	5.15	56.19	56.86	57.49	52.21	52.54	52.81
1383	5.20	56.76	57.42	58.04	52.84	53.16	53.43
1407	5.27	56.87	57.53	58.14	52.97	53.29	53.55
1437	5.35	56.87	57.53	58.14	52.63	52.94	53.20
1485	5.48	56.87	57.53	58.14	51.93	52.24	52.50
1564	5.70	56.87	57.53	58.14	51.22	51.52	51.78
1625	5.87	56.87	57.53	58.14	50.60	50.90	51.15
1661	5.96	56.87	57.53	58.14	49.95	50.25	50.50
1687	6.04	57.43	58.09	58.69	50.48	50.77	51.02
1709	6.10	58.94	59.58	60.18	52.13	52.41	52.65
1729	6.15	59.90	60.53	61.12	53.19	53.48	53.71
1750	6.21	60.38	61.00	61.58	53.76	54.04	54.27
1775	6.28	60.44	61.06	61.63	53.84	54.11	54.34
1806	6.36	60.44	61.06	61.63	53.84	54.11	54.34

[a]Days from 1 May at Age 1+; [b]1 December

Comparisons to existing models

Many attempts have been made to model seasonal krill growth patterns (e.g. Bargmann 1945, Mackintosh 1972). In the earlier days, growth patterns were based on assumptions of 2 to 3 yr life cycles; therefore, here we mainly compare our results with 2 frequently cited seasonal growth models that used a modified VB growth curve. Siegel (1986) applied a modified VB formula described by Pauly & Gaschutz (1979) and estimated parameters to fit seasonally oscillating length-at-age data derived from length frequency distribution mixture analysis, and suggested a 6 yr life span reaching a population-average length of approximately 57 mm at Age 6 (Fig. 8).

We fitted their model as Eq. (4) to 'pseudo-data' extracted from the growth trajectory obtained by projecting from an average length of 28 mm at 1 December in the second summer of the lifecycle using IGR and IMP models, allowing for negative predictions of IGR. The fit of this model shown in Fig. 8 was reasonably good apart from high amplitude sinusoidal components in the spring and following winter of 1+ and 2+ yr old krill, which poorly predicted zero growth of the IGR/IMP based trajectory for these periods. For Age 5+ yr krill at the end of the summer growth period, the Scenario Ib trajectory and model SVB(Ib) gave an average length close to 53 mm.

Rosenberg et al. (1986) used their PVB model, described in this study by Eq. (5), to demonstrate that it takes at least 6 to 7 yr to reach 60 mm (Fig. 9). However, the PVB growth model was not used to model the Scenario Ia trajectory because it could not adequately capture the rapid increase in length over the summer growth period. Instead, we used a simple empirical model based on the cumulative *F*-distribution that does capture this fast growth, as seen in Fig. 9. Fig. 9 shows that the Rosenberg et al. (1986) model does not provide a smoothed trend that follows the Scenario Ia trajectory. In winter, the length of the Age 1+ yr old krill predicted by the PVB model was as much as 6 to 8 mm above our expected starting value of 28 mm, whereas by Age 5+ yr the PVB model predicted a mean length lower than the Scenario Ia value by about 1.5 mm. If the Scenario Ib IGR/IMP generated trajectory best reflects average growth for the Indian Ocean sector, then the smaller mean length predicted at Age 5+ yr of about 53 mm, compared to Siegel (1986) and Rosenberg et al.'s (1986) predictions for this age (close to 56 mm), could be explained by different levels of food availability and quality between the Indian Ocean and southwest Atlantic sectors. It is generally thought that the Antarctic Peninsula area is more productive than the Indian Ocean sector (e.g. Constable

et al. 2003). However, if the Scenario Ia IGR/IMP generated trajectory best reflects average growth for the Indian Ocean sector, then this provided a similar and even slightly higher mean length-at-Age 5+ yr of about 57.5 mm compared to predictions for the southwest Atlantic sector.

Rosenberg et al. (1986) and Siegel (1986) calibrated their VB models using age-cohort modal lengths estimated from length frequency data (LFD). The shift in age-cohort modal length between consecutive LFD samples for a sequence of sampling times was used to infer the growth of this cohort over the time period between samples, and was modelled as a function of its estimated age using the VB growth model. The estimated age corresponding to each modal length was inferred from the number of modes extracted from the LFD. Controversy underlies these approaches because they require an assumption that the series of length data used originate from the same homogeneous population. However, for many open-ocean or shelf species, there is no certainty that the same population is being sampled from one survey to the next; in the Antarctic, the prevailing theory is that Antarctic krill are subject to flux and are moved quite rapidly from one area to another (Nicol 2000). When a particular age class is missing or poorly represented, then misclassification of a complete length class or unknown age components of a length class make accurate estimation of age class modal lengths from LFD fraught with difficulty (Reid 2001). Estimation of seasonal patterns of growth represents an extra challenge for LFD analysis (Rosenberg et al. 1986, Reid 2001).

An advantage of our growth model is that the growth trajectory was generated using actual observations of individual animal growth in the field (i.e. the IGR data) and observations on IMP (albeit in controlled environments in this last case). Therefore, our growth model was not subject to between-sample variance and potential bias from inferring growth from the shifts in modal length from LFD. In addition, seasonal variation in growth can be directly quantified using IGR data.

Hoffman & Lascara (2000) developed a time-dependent, size-structured, bioenergetically-based krill growth model. This model allows simulation of the time-dependent growth of krill that are exposed to a range of environmental conditions. Energetically-based growth models are a powerful tool for testing various hypotheses on metabolic processes, and allow evaluation of the processes by which krill over-winter (Hoffman & Lascara 2000). Hoffman & Lascara (2000) demonstrated winter shrinkage dependent on different food conditions and also rapid growth during the spring bloom season, which agrees with our growth trajectory including winter shrinkage generated in this study.

Generalization of IGR growth model

The growth trajectory Scenario Ib (see Fig. 8), we believe, is a reasonably accurate representation of population-average length both across and within years. This could be used as a specified length-at-age vector in krill assessments using the GYM (Constable & de la Mare 1996, 2003), which would be the preferred form of implementing these results. The model based on the *F*-distribution given by Eq. (6) satisfactorily expressed the seasonal growth trajectory when negative growth did not occur (Scenario Ia) as seen in Fig. 9, and either the length-at-age vector or Eq. (6) could be used directly in management software without any appreciable loss of accuracy in the latter case.

The major problem with Rosenberg et al.'s (1986) model is that it shows unrealistically large size for Age 1+ yr krill (35.5 mm) and 2+ yr krill (44.5 mm), compared to the size-at-age derived from various field surveys (Table 1). Another point worth noting here is that, as explained in the introduction, trajectories were generated using only juvenile and male growth estimates. Since mature females were observed to show lower growth rates in late summer (Kawaguchi et al. 2006), if female growth were to be taken into account, then the growth trajectory in the late summer could be slightly moderated for the population as a whole, compared to that currently modelled.

Implications for krill resource management

Krill growth is an important parameter in estimating precautionary catch limits for krill by the Commission for the Conservation of Antarctic Marine Living Resources (CCAMLR). Currently, the GYM (Constable & de la Mare 1996, 2003) is used to implement these assessments. The GYM numerically integrates a set of differential equations that incorporate functions that specify growth, mortality, and recruitment. The primary output of the GYM is an estimate of gamma, which is the proportion of exploitable biomass to unexploited biomass (B_0). The reason why a growth model (especially its seasonal pattern) is so important for management is because the timing of the biomass survey in relation to seasonal growth phases affects the estimate of gamma. For example, if the biomass survey was conducted at the end of the growing period, the estimate of gamma would be smaller than if the same biomass was estimated from a survey earlier in the growth period, since this krill population would increase its biomass towards the end of the growth period.

Currently, the PVB model of Rosenburg et al. (1986) (Fig. 9) is that used in the assessment of yield. The

growth model derived in this study is based on actual growth measurements of individual krill from the Indian Ocean sector of the Southern Ocean, and reflects the seasonal growth pattern in the field. We strongly believe that using the IGR based growth model implemented as a length-at-age vector in the assessment will contribute to improved estimation of the potential yield of the krill stock, which will in turn lead to improved management of the Antarctic marine ecosystem.

Siegel (1986) cited that the main growth period in the Antarctic Peninsula region (southwest Atlantic sector) occurs between October and early January, and that from January onwards he could not detect any further increase in mean length-at-age, not even in the fast growing juvenile Age 1+ yr class. Reid (2001) generated a krill growth trajectory by using seasonal change of length frequency of krill in the fur seal diet at South Georgia, and suggested that while the rapid growth period of krill is between September and December, they grow very little in size from January onwards. Although these studies were based on seasonal LFD analyses, they are in agreement with the seasonal IGR trend for the southwest Atlantic sector provided by Kawaguchi et al. (2006), which showed very little growth in January and February. Given that the period December to January is likely to be the rapid growth period in the Indian Ocean sector, the timing of the growth period appears to be a few months earlier in the southwest Atlantic sector. This inference is supported by the idea that the spring phytoplankton bloom shifts with respect to the ice-edge position (Lancelot et al. 1993) so that the timing of the spring ice-edge phytoplankton bloom in lower latitudinal areas such as the southwest Atlantic occurs earlier compared to the Indian Ocean sector where the latitude is higher. Therefore, it is also important that the application of this seasonal growth model to different areas should be accompanied by phase adjustments according to corresponding periods of rapid growth.

Future model refinements

As mentioned earlier, the IGR database used to develop this model did not have complete seasonal coverage: data were not available for the early spring and winter periods. In order to generate a year-round pattern in growth, we had to make some assumptions about the beginning of the growth period. In addition, we had to make assumptions about winter and early spring IGR, and our predictions of IMP for this period involved an extrapolation of the IMP model to lower temperatures than those used in the published studies that were used for model fitting. Therefore, in order to be confident that the growth trajectories we have generated are realistic—particularly with respect to the prevalence and degree of shrinkage—it is necessary to increase the seasonal coverage of IGR sampling to encompass winter and spring. Increasing the areal coverage is also essential, especially the coverage of the southwest Atlantic sector where most krill fishing is conducted.

Both food and temperature conditions change with season. Therefore, seasonal trends in IGR and IMP in the current model were influenced by the combined effect of these 2 factors. Delineation of the effects of these 2 factors on IGR and IMP would allow us to simulate growth patterns for krill under different environmental conditions. Also, we do not know if there is any trade off between IMP and IGR in krill. It is generally known for crustaceans that frequent moulting is accompanied by reduced IGR (Hartnoll 2001); however, this has not yet been studied for krill. Solving each of these questions through experiments under controlled environments will contribute to further improvements in the model. In addition, conducting these studies of growth and IMP for temperature ranges relevant to all seasons for each of the major sectors of the krill fishery is a high priority.

The current model does not include female IGR as their growth pattern during the summer season is physiologically complex, possibly due to resource distribution into reproductive rather than somatic growth (Kawaguchi et al. 2006). Interestingly, under experimental conditions, females were shown to shrink in size once they finish their reproductive season and began to regress their external sexual characteristics, regardless of feeding condition (Thomas & Ikeda 1987). Incorporation of the effects of sexual maturity and breeding condition on growth should also be considered in the future.

Finally, our model only provides a growth trajectory for population-average length-at-age, and at present we are unable to predict the distribution of lengths about these averages. We can estimate the variance in IGR given pre-moult TL and season, but the generation of realistic distributions for length-at-age requires models calibrated from data that are currently unavailable. These data include measurements of IGR for consecutive moults for individual animals, which requires non-destructive experiments on captive krill and joint measurement of IMP and IGR for these experimental animals. When we assumed that consecutive IGRs are independent of each other and independent of IMP, the predicted 95% population limits of the length-at-age distribution we obtained gave unrealistically large krill at Age 5+ yr for the upper limit and rather small krill at this age for the lower limit. Therefore, obtaining this type

of data from non-destructive captive rearing experiments using a range of temperature and feeding regimes would be an important advance in our understanding and ability to model the growth of Antarctic krill.

CONCLUSIONS

For the first time, the growth trajectory for length of Antarctic krill was generated using a model based on IGR data accumulated over a period of more than 10 yr. Our new approach allowed us to incorporate winter shrinkage into the model and also successfully generalized the seasonal growth pattern by fitting a seasonal VB growth model (Pauly & Gaschutz 1979, Siegel 1987). Our models indicated that, allowing for shrinkage, the Age 5+ yr mean length at the end of the summer growth period for the Indian Ocean sector was close to 53 mm, compared to 56 mm obtained from studies for the southwest Atlantic sector. A growth scenario that did not include winter shrinkage predicted a mean length at this age of 57.5 mm. Both of the proposed generalized IGR models reproduced the pattern of rapid summer growth that is likely to occur in the natural environment. We believe that application of these growth models to the current krill management model will contribute to further improvement of the krill ecosystem-based management system.

Acknowledgements. We are grateful to A. Constable for reviewing this paper and to S. Nicol for valuable comments. Thanks are extended to anonymous reviewers whose comments improved the manuscript.

LITERATURE CITED

Aseev YP (1984) Size structure of krill populations and life span in the Indian Ocean Sector of the Antarctic. Hydrobiology 6:89–94

Bargmann HE (1945) The development and life-history of adolescent and adult krill *Euphausia superba*. Discov Rep 23:103–176

Buchholz F (1991) Moult cycle and growth of Antarctic krill *Euphausia superba* in the laboratory. Mar Ecol Prog Ser 69:217–229

Butler D, Cullis BR, Gilmour AR, Gogel BJ (2002) Spatial analysis mixed models: samm reference manual, training series QE02001. Queensland Department of Primary Industries, Toowoomba

CCAMLR (2000) Report of the working group on ecosystem monitoring and management. SC-CAMLR XIX, Annex 4

Constable AJ, de la Mare WK (1996) A generalized model for evaluating yield and the long-term status of fish stocks under conditions of uncertainty. CCAMLR Sci 3:31–54

Constable AJ, de la Mare WK (2003) Generalised yield model, version 5.01b. Australian Antarctic Division, Kingston

Constable AJ, Nicol S, Strutton PG (2003) Southern Ocean productivity in relation to spatial and temporal variation in the physical environment. J Geophys Res 108:6–21

Dallwitz MJ, Higgins JP (1992) User's guide to DEVAR. A computer program for estimating development rate as a function of temperature. CSIRO Aust Div Entomol Rep 2: 1–23

Grose M, McMinn A (2003) Algal biomass in east Antarctic pack ice: how much is in the east? In: Huiskes AHL, Gieskes WWC, Rozema J, Schorno RML, van der Vies SM, Wolff WJ (eds) Antarctic biology in a global context. Backhuys Publishers, Lieden, p 21–25

Hartnoll RG (2001) Growth in crustacea—twenty years on. Hydrobiologia 449:111–122

Hoffman EE, Lascara CM (2000) Modeling the growth dynamics of Antarctic krill *Euphausia superba*. Mar Ecol Prog Ser 194:219–231

Hosie GW, Ikeda T, Stolp M (1988) Distribution, adundance and population structure of the Antarctic krill (*Euphausia superba* Dana) in the Prydz Bay region, Antarctica. Polar Biol 8:213–224

Ikeda T, Dixon P (1982) Body shrinkage as a possible overwintering mechanism of the Antarctic krill, *Euphausia superba* Dana. J Exp Mar Biol Ecol 62:143–151

Jacques G, Fukuchi M (1994) Phytoplankton of the Indian Antarctic Ocean. In: El-Sayed S (ed) Southern Ocean ecology: the BIOMASS perspective. Cambridge University Press, Cambridge, p 63–78

Kawaguchi S, Candy SG, King R, Naganobu M, Nicol S (2006) Modelling growth of Antarctic krill. I. Growth trends with sex, length, season, and region. Mar Ecol Prog Ser 306: 1–15 (this volume)

Lancelot C, Mathot S, Veth C, de Baar H (1993) Factors controlling phytoplankton ice-edge blooms in the marginal ice-zone of the northwestern Weddell Sea during sea ice retreat 1988: field observations and mathematical modelling. Polar Biol 13:377–387

Lu B, Wang R (1996) Further study on distribution mixture analysis and its application to age-groups analysis of Antarctic krill. Oceanol Limnol Sin 27:179–186

Mackintosh NA (1972) Life cycle of Antarctic krill in relation to ice and water conditions. Discov Rep 36:1–94

Nicol S (2000) Understanding krill growth and aging: the contribution of experimental studies. Can J Fish Aquat Sci 57: 168–177

Nicol S, Stolp M, Cochran T, Geijsel P, Marshall J (1992) Growth and shrinkage of Antarctic krill *Euphausia superba* from the Indian Ocean sector of the Southern Ocean during summer. Mar Ecol Prog Ser 89:175–181

Pakhomov EA (1995) Demographic studies of Antarctic krill *Euphausia superba* in the Cooperation and Cosmonaut Seas (Indian sector of the Southern Ocean). Mar Ecol Prog Ser 119:45–61

Pauly D, Gaschutz G (1979) A simple method for fitting oscillating length growth data with a program for pocket calculators. ICES Demersal Fish Cttee, Ref Pelagic Fish Cttee CM 1979/G:24

Quetin LB, Ross RM (1991) Behavioural and physiological characteristics of the Antarctic krill, *Euphausia superba*. Am Zool 31:49–63

Quetin LB, Ross RM, Clarke A (1994) Krill energetics: seasonal and environmental aspects of the physiology of *Euphausia superba*. In: El-Sayed S (ed) Southern Ocean ecology: the BIOMASS perspective. Cambridge University Press, Cambridge, p 165–184

Reid K (2001) Growth of Antarctic krill *Euphausia superba* at South Georgia. Mar Biol 138:57–62

Rosenberg AA, Beddington JR, Basson M (1986) Growth and longevity of krill during the first decade of pelagic whaling. Nature 324:152–154

Ross RM, Quetin LB, Baker KS, Vernet M, Smith RC (2000) Growth limitation in young *Euphausia superba* under field conditions. Limnol Oceanogr 45:31–43

Siegel V (1986) Untersuchungen zur Biologie des antarktischen Krill, *Euphausia superba*, im Bereich der Bransfield Straße und angrenzender Gebiete. Mitt Inst Seefisch 38:1–244

Siegel V (1987) Age and growth of Antarctic Euphausiacea (Crustacea) under natural conditions. Mar Biol 96:483–495

Stinner RE, Gutierrez AP, Butler Jr GD (1974) An algorithm for temperature-dependent growth rate simulation. Can Entomol 106:519–524

Stinner RE, Butler GD Jr, Bacheler JS, Tuttle C (1975) Simulation of temperature-dependent development in population dynamics models. Can Entomol 107:1167–1174

Thomas PG, Ikeda T (1987) Sexual regression, shrinkage, re-maturation and growth of spent female *Euphausia superba* in the laboratory. Mar Biol 95:357–363

Verbyla AP, Cullis BR, Kenward MG, Welham SJ (1999) The analysis of designed experiments and longitudinal data using smoothing splines (with discussion). Appl Stat 48: 269–311

Wang R, Lu B, Li C, Wang W, Ji P (1995) Age-groups of Antarctic krill (*Euphausia superba* Dana) by distribution mixture analysis from length-frequency data. Oceanol Limnol Sin 26:598–605

Editorial responsibility: Otto Kinne (Editor-in-Chief), Oldendorf/Luhe, Germany

Submitted: May 26, 2005; Accepted: October 13, 2005
Proofs received from author(s): December 7, 2005